RSC Advances

ROYAL SOCIETY
OF CHEMISTRY

www.rsc.org/advances

RSC Advances

ARTICLE

WS₂ nanoparticles - potential replacement for ZDDP and friction modifier additives

M. Ratoi,*[a] V. B. Niste[a] and J. Zekonyte[a]

In high-pressure, high-temperature sliding contacts, WS₂ nanoadditives react with the metal substrate to generate 100+ nm chemical tribofilms with a layered structure and excellent tribological properties. The friction, wear and micromechanical properties of WS₂ tribofilms are compared with those of tribofilms formed by the zinc dialkyldithiophosphate (ZDDP) antiwear additive and ZDDP-organic friction modifier (OFM) mixture. Nanoindentation measurements showed that WS₂ generates tribofilms with higher values of hardness and Young's modulus than ZDDP and ZDDP+OFM, which explains its excellent antiwear properties. The friction performance of WS₂ surpassed that of ZDDP+OFM. The striking reduction of boundary friction is credited to the layered structure of the WS₂ tribofilm, with exfoliated/squashed WS₂ nanoparticles that fill the gaps and cover the reacted tribofilm. In view of these results, WS₂ proves to be a suitable candidate for the replacement of problematic lubricant additives currently in use.

1. Introduction

Integration of nanoscale materials into tribological systems has been enthusiastically driven over the last two decades by their wide range of potential benefits. In lubricants (such as engine oils, transmission fluids, gear and bearing oils), nanoadditives have the potential to reduce friction and wear of moving parts and enhance machine durability.[1,2] In the case of engine crankcase lubricants, the lower friction can assist in reducing fuel consumption and emission of greenhouse gases, while the potential of nanoparticles (NPs) for low sulphated ash, phosphorous and sulphur (SAPS) vehicle emissions could extend the durability of exhaust treatment devices and offer a roadmap to eco-friendly technology.[3,4] From the myriad of investigated nanoadditives with a view for tribological applications, WS₂ NPs have been shown to supersede other materials that have been traditionally used in lubrication (MoS₂, graphite, Ag, CuS etc.).[5-9] Published research has shown WS₂ NPs to possess remarkable antiwear, extreme pressure, friction and physicochemical properties.[5,6,10-14] These recommend them as potential candidates for replacing problematic additives (such as the antiwear ZDDPs), which are extensively used in lubricants despite their drawbacks.

Conventional lubricant formulations for tribological contacts which work in mixed and boundary lubrication regimes contain a mixture of friction modifiers and antiwear additives. Previous published work has reported that the ubiquitous ZDDP antiwear additives react rapidly with the hot rubbed ferrous surfaces to form thick iron and zinc phosphate-based tribofilms, characterized by low shear strength values.[15,16] Apart from being generally toxic and poisonous to the exhaust catalyst in automotive applications, their main drawback is the high friction values of the generated tribofilms. Friction modifier (FM) additives are added to overcome this inconvenience.

In a previous study we have reported that WS₂ nanoadditives behave similarly to ZDDPs, in that they also react with the metal substrate in high pressure, high temperature contacts to generate antiwear chemical tribofilms. The films have a thickness of 100–200 nm and are composed of tungsten and iron oxides and sulphides. Apart from their excellent antiwear action, WS₂ tribofilms have the added benefit of being capable to reduce friction in mixed and boundary lubrication conditions.[17]

This study investigates and compares the tribological properties of WS₂ nanoadditives, a conventional antiwear additive (ZDDP) and the ZDDP+FM additive mixture. It also examines the micromechanical characteristics of the tribofilms generated by these additives, which account for their antiwear properties. A Mini Traction Machine (MTM) tribometer was employed to measure the friction and wear properties of oils that contain these additives, while the generation and properties of the tribofilms were investigated using the 3D Spacer Layer Imaging Method (MTM-SLIM),[18] Alicona profilometry[19] and nanoindentation.[20]

The results have shown that the tribological performance of WS₂ NPs is similar to each of these categories of additives

when used individually and surpasses that of their mixture with regard to boundary friction reduction. This is ascribed to the characteristics of the WS$_2$ tribofilm.[17]

2.   Materials and methods

The WS$_2$ NPs with a manufacturer measured average size of 90 nm were purchased from M K IMPEX Canada. They were characterized with TEM, EDX, XRD and Raman, and were found to be 2H-WS$_2$ NPs with flat, stacked sheets forming two populations of different morphologies: triangular and hexagonal (Fig. 1)[17].
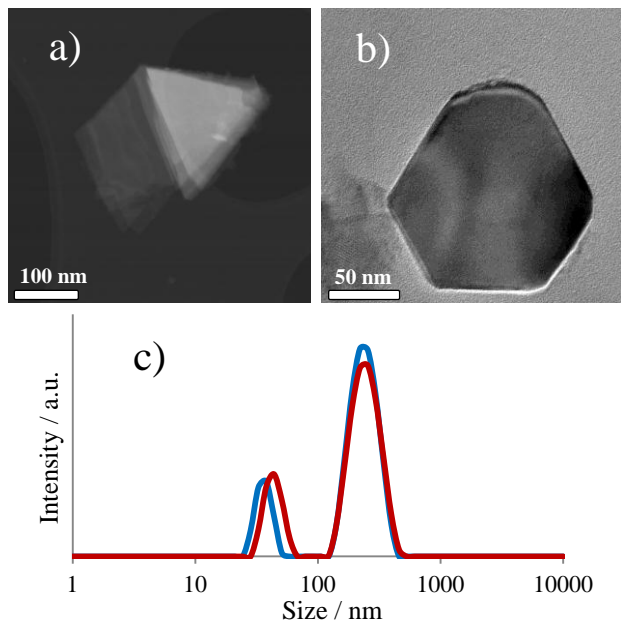

Fig. 1 a, b. TEM pictures showing the two 2H-WS$_2$ (plate-like) nanoparticle morphologies: triangular and hexagonal; c. Particle size distribution for 1 wt % 2H-WS$_2$ NPs in PAO

WS$_2$ NP dispersions in base oil with a concentration of 1 wt % were prepared using a probe sonifier. This concentration has been recommended in published lubrication research as the optimal value.[6,21] To avoid any competition for the nanoadditive to adhere and react with the lubricated metal substrate, the base oil was specifically chosen to have a very low polarity (SpectraSyn Plus 6) and no surfactant/dispersant was used to stabilize the NP dispersions. SpectraSyn Plus 6 (Mobil) is a polyalphaolefin (PAO) which has a density of 830 kg/m^3 at 15ºC and viscosity of 30.3 cSt at 40ºC and 5.9 cSt at 100ºC. The size distribution of the WS$_2$ NPs dispersed in PAO was characterized immediately after preparation by dynamic light scattering (Malvern ZetaSizer Nano ZS). The intensity distribution (Fig. 1) showed the presence of two distinct NP population sizes: one with an average diameter of 40 nm and the other of approximately 250 nm. This particular size distribution of NPs can be potentially beneficial to tribological applications, because it increases their ability to penetrate

contacts and fill asperity gaps of different sizes, thus limiting the adhesion of contact surfaces and reducing friction.

The antiwear additive was a mixed primary/secondary alkyl ZDDP used in 0.4 wt % (1351 ppm phosphorous) in the base oil. An organic friction modifier (OFM) - a straight chain polyamidoalcohol - was added at a 0.5 wt % treat rate. These concentrations of ZDDP and OFM are typical for commercial formulated lubricants.

Tribological tests were carried out in a Mini Traction Machine (MTM) in a sliding-rolling ball-on-disc setup. This features a 19 mm diameter ball and a 46 mm diameter disc, both made of AISI 52100 steel (hardness 750-770 HV). The root-mean-square roughness of both balls and discs is 11 ± 3 nm, resulting in a composite surface roughness of approximately 16 nm. New specimens (balls and discs) were used for each test and were cleaned with solvents (toluene followed by isopropanol) in an ultrasonic bath for 10 minutes prior to the test. Throughout the test, the temperature was kept constant at 100ºC and the applied load was 30 N, corresponding to an initial mean Hertz pressure of 0.94 GPa. The slide-roll ratio (SRR), calculated as the ratio of the sliding speed (u_b-u_d) to the entrainment speed (u_b+u_d)/2 (where u_b and u_d are the speed of the ball and the disc, with respect to the contact) was 150%. This slide-roll ratio value was selected to be higher than in previously reported research[22] to accelerate the generation of the chemically reacted tribofilm, which is known to depend on the severity of the rubbing conditions.[15] During the test, the NP dispersion was maintained at constant temperature in the enclosed, temperature insulated chamber, where it was stirred continuously and vigorously by the circular movements of the disc and ball. Therefore, even in the absence of a surfactant, the NPs were maintained well dispersed and only a small number sedimented at the bottom of the lubricant chamber at the end of the 3 hour test.
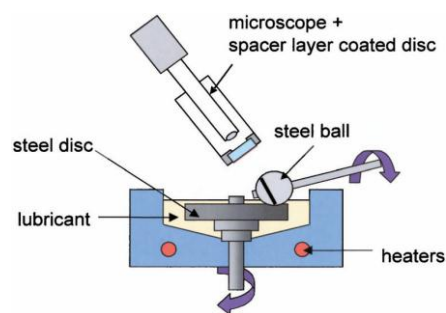
Fig. 2 Diagram of the Mini Traction Machine (MTM) [18]

The MTM is fitted with the 3D Spacer Layer Imaging Method (SLIM) attachment, which enables in situ capture of optical interference images of the tribofilms on the steel ball (Fig. 2) using a high resolution, RGB colour camera. The analysis software matches colours in the image to a calibration file in order to determine the film thickness of every point in the image.[18] The thickness of the tribofilm in each image was calculated as the average value inside a circular area taken across the entire width of the wear track.

The tribological tests followed a routine which can be divided in three alternative stages repeated at fixed time intervals. The

first stage was the '*conditioning phase*', when the ball and disc were rubbed together at a fixed slow entrainment speed in mixed lubrication film conditions to generate a tribofilm on the ball and disc wear track. The following stage consisted of the '*Stribeck curve*' acquisition, in which friction was measured over a range of entrainment speeds at a fixed slide-roll ratio. The acquisition of data for the Stribeck curve started at the highest speed (1.5 m/s) and continued towards the lowest speed (10 mm/s) value, to protect the formed tribofilm by avoiding its damage at low speeds in the boundary regime. The third stage was the '*tribofilm measurement*', when the motion was halted, the spacer layer-coated window was loaded against the ball track and an image was captured. Table 1 summarizes the conditions used for the MTM-SLIM tests in this study.

Table 1 MTM– SLIM test conditions

Conditioning phase	
Temperature	100ºC
Load	30 N
Mean Hertz pressure	0.94 GPa
Entrainment speed	0.1 m/s
Slide-roll ratio (SRR)	150 %
Stribeck curve phase	
Temperature	100ºC
Load	30 N
Mean Hertz pressure	0.94 GPa
Entrainment speed	1.5 to 0.01 m/s
Slide-roll ratio (SRR)	150 %

Thickness profiles of the tribofilms and the width of the wear tracks were measured at the end of the 3 h MTM tests with the Alicona Infinite Focus profilometer[19] (at 20x magnification).

Nanoindentation tests were conducted to characterize the mechanical properties of the tribofilm. Nanoindentation is a depth sensing technique capable of providing measurements of elastic and plastic properties, where the indentation process is continually monitored with respect to force, displacement and time. Nanoindentation of tribofilms was performed to determine the hardness and reduced elastic modulus[23] using a NanoTest Platform 3 instrument (Micro Materials, Wrexham, UK).[20] This pendulum based nanoindentation system is extensively explained in literature.[24]

Indentations were performed using a Berkovich diamond indenter in a depth-controlled mode. Maximum penetration depth depended on tribofilm thickness and was set to 20 or 30 nm. The maximum loading force was 1 mN and the loading and unloading rates were kept constant. The loading and unloading times were set to 20 s and a dwell time of 10 s was selected at maximum load to reduce the influence of creep. A matrix of 100 or 200 indents was imprinted onto the sample surface (15 μm apart, over an area of $150 \times 150 / 300 \times 300$ μm^2) to map the distribution of mechanical properties. The data were analysed using the Oliver and Pharr method[23] with the analytical software provided by instrument manufacturers.

3. Results and discussion

Stribeck curves were measured during a 3-h rubbing test using 1 wt % WS$_2$ NPs in PAO (Fig. 3 a), 0.4 wt % ZDDP in PAO (Fig. 3 b) and 0.4 wt % ZDDP + 0.5 wt % OFM in PAO (Fig. 3 c). The curves illustrate the dynamics of tribofilm growth/removal in time (following various conditioning periods) throughout the mixed and boundary lubrication regimes.
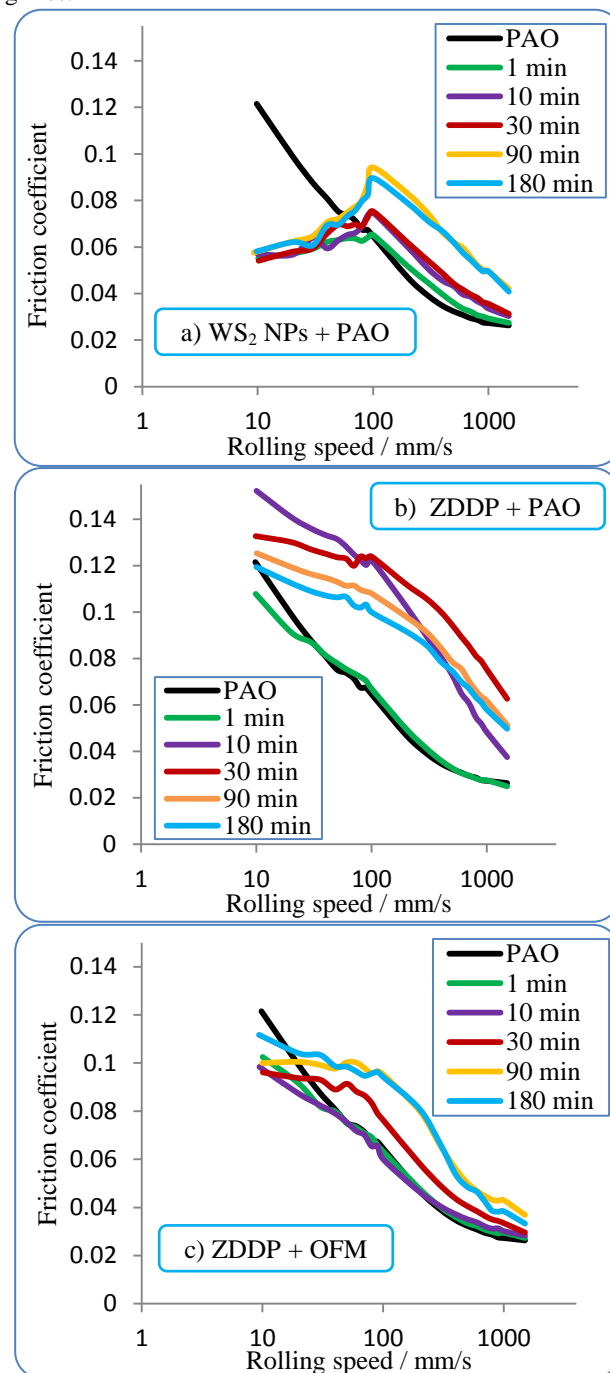

Fig. 3 Stribeck curves for PAO and PAO with additives after 1, 10, 30, 90 and 180 minutes of rubbing at 100ºC: a) 1 wt % WS$_2$ NPs in PAO, b) 0.4 wt % ZDDP in PAO and c) 0.4 wt % ZDDP + 0.5 wt % OFM in PAO
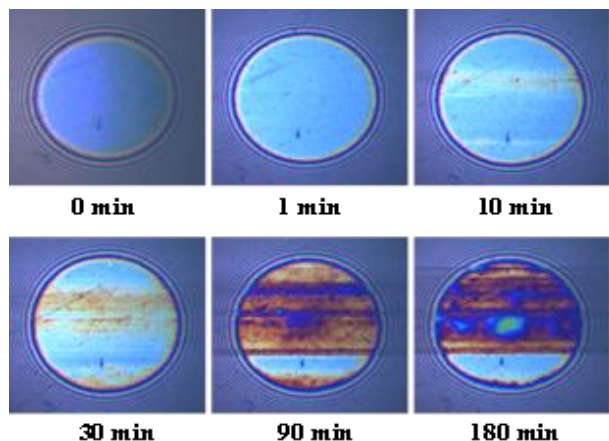
Fig. 4 shows a comparison of the Stribeck curves for the base oil and its blends with the three additives, measured after 3 h of rubbing.
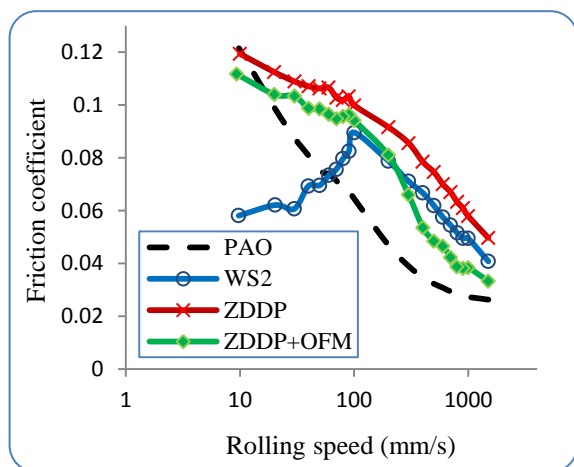
Fig. 4 Stribeck curves for PAO and PAO with additives after 180 minutes of rubbing at 100ºC
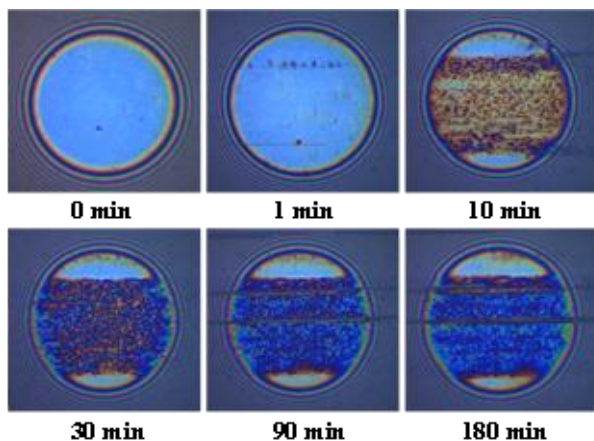
**Fig. 5** Interference images of the ball track during rubbing with ZDDP

Fig. 6 Interference images of the ball track during rubbing with ZDDP+OFM

Fig. 5 and 6 show optical interference images taken during the ZDDP and ZDDP+OFM tests. The sliding direction in all of these images is from left to right. The first image was taken before the test started. The development of the ZDDP antiwear chemical tribofilm on the wear track during rubbing is indicated by the dark areas. The interference images are used to calculate the average tribofilm thickness in the central region. The tribofilm thickness values for ZDDP and ZDDP+OFM lubricants are plotted against time in Fig. 7.

From the results shown in Fig. 3b and 5, it can be seen that the ZDDP lubricant develops a pad-like structure during prolonged rubbing. The film starts to form after approximately 5 minutes of rubbing and during the first 30 minutes, the increase in film thickness can be correlated with the increase in friction. As the test progressed in time, the tribofilms continued to increase in thickness but their friction decreased (as shown by the Stribeck curves measured after 90 and 180 minutes of rubbing). These results can be explained by considering other published results, which showed that the morphology of ZDDP derived tribofilms evolves with rubbing time to become smoother and more uniformly distributed.[15,25]

The current study employed a high SRR (150 %). This resulted in the formation of thicker ZDDP tribofilms (200+ nm) than reported in other published work, which used a SRR of 50 % but otherwise similar testing conditions.[22,26] The SRR was reported to influence tribofilm formation and its characteristics. The tribofilm thickness values result from the balance between the formation rate and removal rate determined by wear.[27,28]

In line with expectations, the addition of OFM to ZDDP decreased friction in the mixed and boundary regimes (Fig. 3 c). However, as shown in Figures 5, 6 and 7, the OFM also reduced the thickness of the ZDDP antiwear tribofilm (204 nm for ZDDP and only 165 nm for ZDDP+OFM) and significantly delayed its formation (ZDDP+OFM only started to generate a tribofilm after approximately 30 minutes of rubbing). These findings are in agreement with other previously published work, in which a mineral oil was used as base oil.[29]
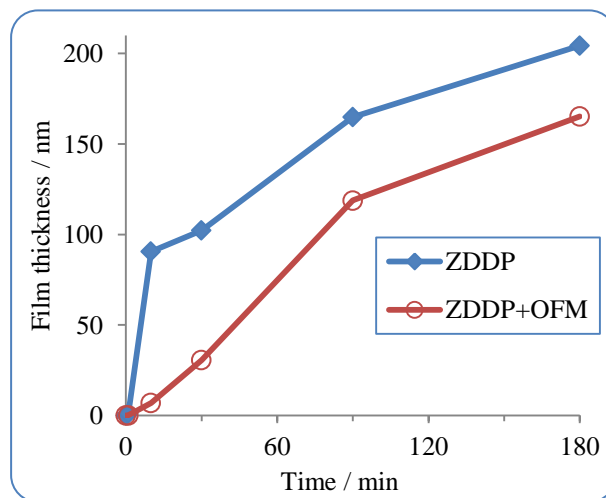

Fig. 7 Growth kinetics of ZDDP and ZDDP+OFM tribofilms

The Stribeck curves for the WS_2 lubricant showed that friction started to increase after 5-7 minutes of rubbing (which can indicate the beginning of tribofilm formation) and continued to gradually rise in the first 90 minutes after which it remained constant until the end of the 3 h test. In the mixed regime (100-1500 mm/s), the friction levels of WS_2 are lower than of ZDDP and are similar to the ZDDP+OFM lubricants.

A significant difference in friction between the three lubricants can be seen in the boundary regime. In the case of ZDDP, friction continues to increase as the speed is reduced, reaching values much higher than that of the base oil. The boundary friction values of the ZDDP+OFM lubricant are considerably lower than for ZDDP and slightly lower than for the base oil. The WS_2 lubricant shows a striking drop in friction with decreasing speed starting at 100 mm/s and reaches friction values of 0.55 at 10 mm/s.

Fig. 8 shows interference images of the ball wear track acquired at the end of the 3 h MTM test for the PAO lubricants containing the three additives. The average tribofilm thickness values were 200 nm for ZDDP, 165 nm for ZDDP+OFM and 100 nm for the WS_2 NPs lubricant.

The thickness of the chemical tribofilm generated by the WS_2 lubricant was measured with the SLIM system only at the end of the 3 h test. During the test, the WS_2 NPs adhered to the spacer layer-coated window and impeded the imaging of the tribofilm. At the end of the test the window and the wear track were cleaned and an image of the tribofilm was acquired (Fig. 8 a).


a) 100 nm   b) 200 nm   c) 165 nm
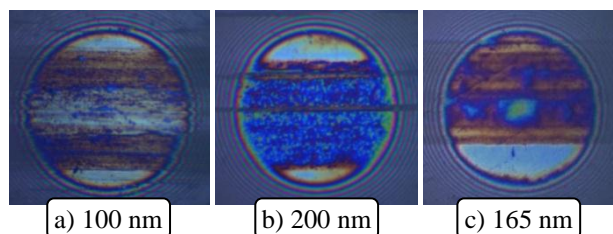
Fig. 8 Interference images of the ball track after 3 h rubbing with a) WS_2 NPs, b) ZDDP and c) ZDDP+OFM
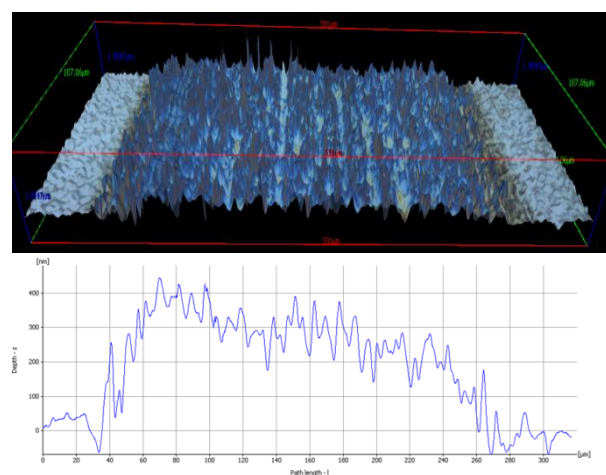
Alicona images and profiles of the tribofilms formed on the MTM discs reveal their specific morphology (Fig. 9, 10 and 11). The height axis was increased 20 times for a clearer view. The calculated average height of the tribofilms measured with SLIM on the MTM balls and Alicona on the MTM discs were similar (Table 2). The slightly lower thickness values measured *in situ* with the SLIM system are the result of the tip asperities being flattened under the high contact pressure.

Table 2 Average thickness values (nm) of chemically reacted tribofilms after 3h rubbing at 100 °C

	WS_2	ZDDP	ZDDP + OFM
SLIM (ball)	98	204	165
Alicona (disc)	109	245	180
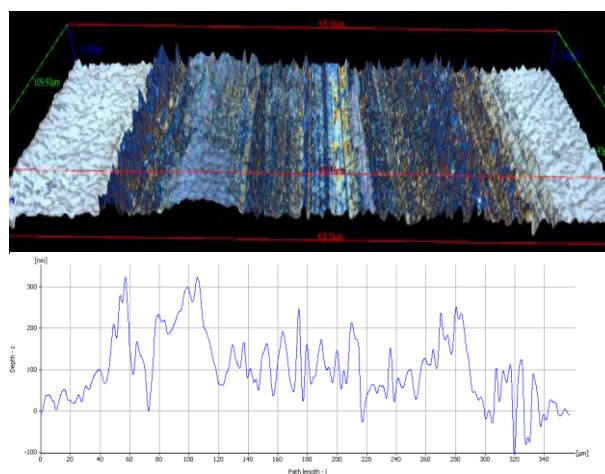
Fig. 9 3D Alicona image of the WS_2 NPs tribofilm and profile view across the track

Fig. 10 3D Alicona image of the ZDDP tribofilm and profile view across the track
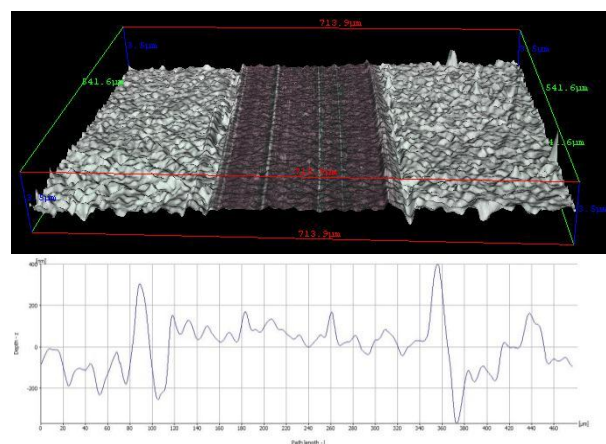
Fig. 11 3D Alicona image of the ZDDP+OFM tribofilm and profile view across the track

The antiwear properties of the additives were assessed by measuring the width of the disc wear track at the end of the 3 h test with the Alicona profilometer. Wear loss determinations

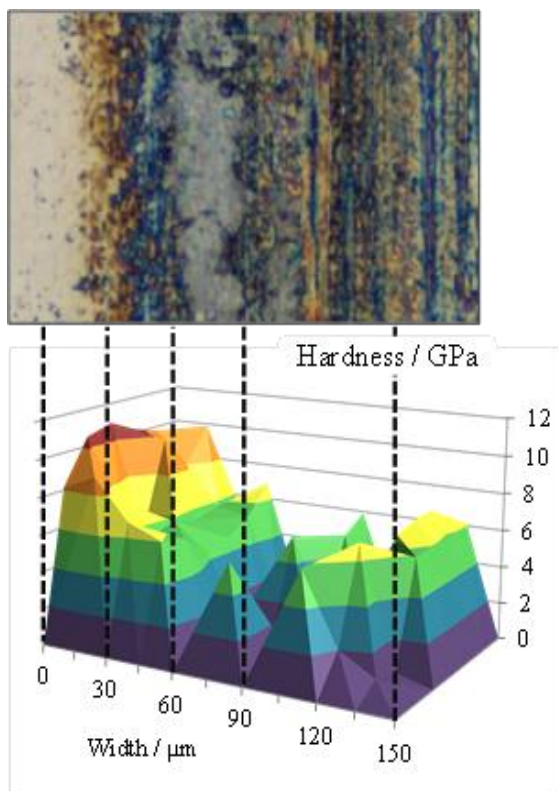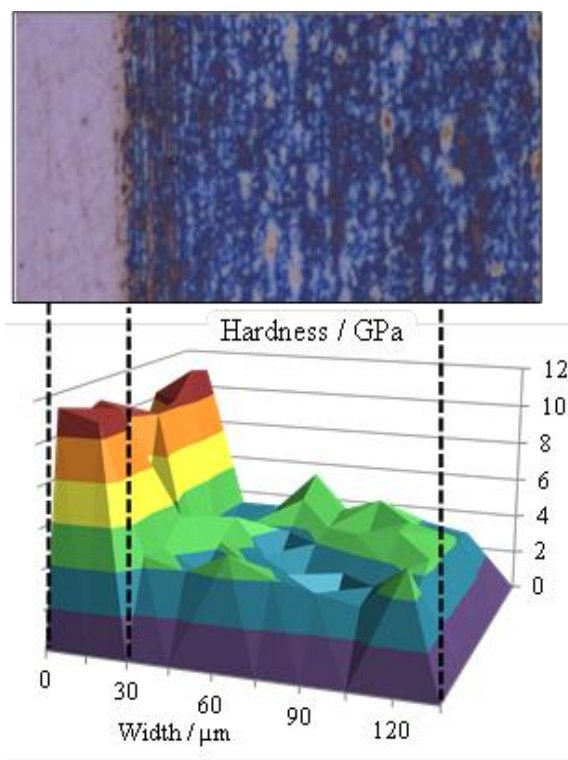were not possible because the tribofilms were above the surface level. The width of the ZDDP wear track was approximately 240 μm. A similar value (250 μm) was measured for the WS_2 NPs and ZDDP+OFM. Although the tests were carried out for only three hours, the results indicate that the antiwear properties of the WS_2 NPs are similar to the ZDDP and ZDDP+OFM additives.

Micromechanical properties (hardness, H, and reduced Young modulus, E') of the tribofilms generated by WS_2, ZDDP and ZDDP+OFM lubricants were measured using nanoindentation.

The depth of nanoindentation was 20-30 nm, depending on the tribofilm thickness. Measurements were performed on the thickest part of the tribofilm (film of approximately 200-250 nm) to reduce the influence of the steel substrate. According to data from published literature, to avoid the effects of the substrate on the determination of thin film mechanical properties, the depth of nanoindentation should be maximum 10% of its thickness when measuring the reduced Young modules and 20% when measuring hardness.[30] The depth of indentation in our study is 12-17% of the measured tribofilm thickness, which indicates that the hardness results are correct but the reduced Young's modulus results may be slightly higher than the actual values.

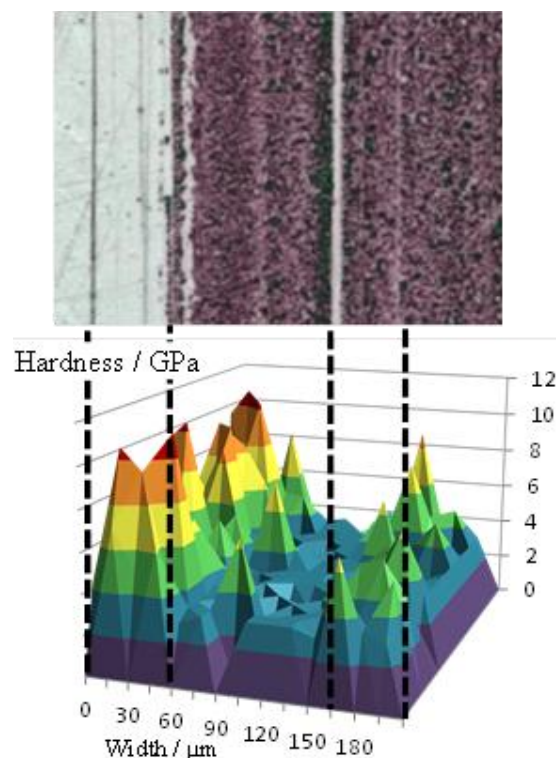Nanoindentation tests of the steel substrate were also performed outside the wear track for comparison. The analysis started outside the tribofilm and continued towards its centre.

Fig. 13 Map of nanoindented sections of steel and tribofilm for ZDDP

Fig. 12 Map of nanoindented sections of steel and tribofilm for WS_2

Fig. 14 Map of nanoindented sections of steel and tribofilm for ZDDP+OFM

Fig. 12 shows that the WS_2 tribofilm presents four distinctive sections: section 1 (0-30 μm)—steel; section 2 (30-60 μm)—chemically formed tribofilm; section 3 (60-90 μm)—chemically formed tribofilm covered with a thick layer of unreacted, squashed WS_2 NPs and section 4 (90+ μm)—chemically formed tribofilm with a few NPs.

The chemically formed tribofilm (section 2 in Fig. 12) is characterized by high H (5.8 ± 0.6 GPa) and E' (166 ± 19 GPa) values, as a result of its unique chemical composition. The tribofilm was investigated with XPS and SIMS and found to have a layered structure. The upper part was found to be composed of unreacted WS_2 sheets and/or squashed WS_2 NPs (the layer is approx. 200 nm), WO_3, iron oxides and sulphides, while the deeper layers and the interface with the steel substrate consist of WO_3 and elemental tungsten and iron.[17]

In comparison to WS_2, the Alicona image and profile as well as the hardness mapping (Fig. 10 and Fig. 13) show that the ZDDP tribofilm is more uniform in thickness and hardness values, although the hardness is lower than that of the reacted WS_2 film (Tab. 3). Addition of the OFM to ZDDP resulted in the formation of an even more uniform but softer tribofilm (Fig 11 and Fig. 14).

Table 3 H and E' values obtained by nanoindentation

	H (GPa)	E' (GPa)
Steel substrate	9.5 ± 0.9	197 ± 10
WS_2 tribofilm	5.8 ± 0.6	166 ± 19
ZDDP tribofilm	4.3 ± 1.0	140 ± 24
ZDDP+OFM tribofilm	3.2 ± 1.8	85 ± 57

Table 3 shows the hardness and reduced Young's modulus values measured for steel substrate and the ZDDP, ZDDP+OFM and WS_2 (section 2 in Fig. 12) chemical tribofilms.

The H and E' values of ZDDP tribofilms are comparable with those reported by other research studies (H = 5 GPa and E' = 110 GPa)[31] and are higher than for ZDDP+OFM tribofilms. The OFM therefore influenced not only the thickness and generation kinetics of the ZDDP tribofilm (as shown in Fig. 6 and 7), but also reduced the mechanical properties of the chemical tribofilm. These findings prove that the OFM has interfered with the ZDDP tribofilm formation. The H and E' values of the WS_2 tribofilm are higher than those of the ZDDP and ZDDP+OFM tribofilms and much larger than the reported values of MoDTC tribofilms, H = 0.4 GPa and E' = 10 GPa.[32] These values imply and that the presence of tungsten in the chemical composition of the WS_2 tribofilms enhances its mechanical properties and grants the excellent antiwear and extreme pressure behaviour reported by many studies.

The chemical tribofilm generated by WS_2 NPs has thickness and morphology similar to the ZDDP and ZDDP+OFM films, but it is covered with platelet-like 2H-WS_2 NPs. These exert a levelling and smoothing effect of the rough areas of the chemical tribofilm and thus significantly lower the boundary friction.

Although the WS_2 nanoadditive is less economical than the related and widely used metal chalcogenide MoS_2, it offers the advantage of the formation of a chemically reacted hard tribofilm characterized by both good antiwear properties and persistent low friction. It has been shown that molybdenum compounds (like MoS_2 and MoDTC), used alone or in combination with ZDDP in oils leads to the formation of abrasive MoO_3, which is conducive to high friction.[33]

Conclusions

In the testing conditions employed in this study, WS_2 NPs generated chemical tribofilms similar to ZDDPs. The tribofilms were 100+ nm in thickness and started forming after approximately 5 minutes of rubbing.

Compared to ZDDP+OFM, WS_2 generated tribofilms much faster and these showed a superior ability to decrease the friction in the boundary regime.

WS_2 tribofilms have a layered structure, with the upper part composed of unreacted WS_2 sheets and/or squashed WS_2 NPs, WO_3, iron oxides and sulphides, while the deeper layers and the interface with the steel substrate consist of WO_3 and elemental W and Fe.

The presence of elemental tungsten and tungsten oxide in the WS_2 chemically reacted tribofilm enhances its mechanical properties, as evidenced by the hardness and elastic modulus values and may explain the excellent antiwear and extreme pressure behaviour reported by numerous published studies.

Although WS_2 tribofilms are comparable in thickness, morphology and antiwear properties to those generated by ZDDP antiwear additives, their peculiarity is the ability to instantly reduce friction to very low values in boundary lubrication. This friction modifying action is credited to the exfoliated and squashed 2H-WS_2 NPs, which fill the gaps and cover the reacted patchy tribofilm to exert a smoothing, low friction effect.

WS_2 NPs have the advantage of reducing both friction and wear in hot rubbing contacts and show great potential for replacement of the popular, but problematic additives in use.

Notes and references

[a] National Centre for Advanced Tribology, University of Southampton, UK

1 V. N. Bakunin, A. Y. Suslov, G. N. Kuzmina, O. P. Parenago, Synthesis and application of inorganic nanoparticles as lubricant components – a review, *J. Nanopart. Res.*, 2004, **6** (2), 273-284.

2 J. M. Martin, N. Ohmae, Nanoparticles made of metal dichalcogenides, In *Nanolubricants*; Volume 13 of Tribology in Practice Series, John Wiley & Sons: Chichester, 2008, 15-40.

3 N. Canter, Special report: Additive challenges in meeting new automotive engine specifications, *Tribol. Lubr. Technol.*, 2006, 10-19

4 H. A. Spikes, Low- and zero-sulphated ash, phosphorous and sulphur anti-wear additives for engine oils, *Lubr. Sci.*, 2008, **20** (2), 103-136.

5 O. Tevet, P. Von-Huth, R. Popovitz-Biro, R. Rosentsveig, H. D. Wagner, R. Tenne, Friction mechanism of individual multi-layered nanoparticles, *Proc. Natl. Acad. Sci. U. S. A., Early Ed*, 2011, **108** (50), 19901-19906.

6 F. Abate, V. D'Agostino, R. Di Giuda, A. Senatore, Tribological behaviour of MoS2 and inorganic fullerene-like WS2 nanoparticles under boundary and mixed lubrication regimes, *Tribology*, 2010, **4** (2), 91-98.

7 X. Kang, B. Wang, L. Zhu, H. Zhu, Synthesis and tribological property study of oleic acid-modified copper sulfide nanoparticles, *Wear*, 2008, **265**, 150-154.

8 C. G. Lee, Y. J. Hwang, Y. M. Choi, J. K. Lee, C. Choi, J. M. Oh, A study on the tribological characteristics of Graphite Nano Lubricants, *Int. J. Precis. Eng. Manuf.*, 2009, **10** (1), 85-90.

9 Y. Choi, Y. Hwang, M. Park, J. Lee, C. Choi, M. Jung, J. Oh, J. E. Lee, Investigation of Antiwear and Extreme pressure properties of nano-lubricant using graphite and Ag nanoparticles, *J. Nanosci. Nanotechnol.*, 2011, **11** (1), 560-565.

10 R. Tenne, M. Redlich, Recent progress in the research of inorganic fullerene-like nanoparticles and inorganic nanotubes, *Chem. Soc. Rev.*, 2010, **39** (5), 1423-1434.

11 L. Rapoport, Yu. Bilik, Y. Feldman, M. Homyonfer, S. B. Cohen, R. Tenne, Hollow nanoparticles of WS2 as potential solid-state lubricants, *Nature*, 1997, **387**, 791-793.

12 L. Rapoport, V. Leshchinsky, I. Lapsker, Yu. Volovik, O. Nepomnyashchy, M. Lvovsky, R. Popovitz-Biro, Y. Feldman, R. Tenne, Tribological properties of WS2 nanoparticles under mixed lubrication, Wear, 2003, **255** (7), 785-793.

13 L. Rapoport, O. Nepomnyashchy, I. Lapsker, A. Verdyan, A. Moshkovich, Y. Feldman, R. Tenne, Behaviour of fullerene-like WS2 nanoparticles under severe contact conditions, *Wear*, 2005, **259** (1-6), 703-707.

14 C. Shahar, D. Zbaida, L. Rapoport, H. Cohen, T. Bendikov, J. Tannous, F. Dassenoy, R. Tenne, Surface functionalization of WS2 fullerene-like nanoparticles, *Langmuir*, 2010, **26** (6), 4409-4414.

15 M. Aktary, M. T. McDermott, G. A. McAlpine, Morphology and nanomechanical properties of ZDDP antiwear films as a function of tribological contact time, *Tribol. Lett.*, 2001, **12** (3), 155-162.

16 Yu. R. Li, G. Pereira, M. Kasrai, P. R. Norton, The effect of steel hardness on the performance of ZDDP antiwear films: a multi-technique approach, *Tribol. Lett.*, 2008, **29**, 201-211.

17 M. Ratoi, V. B. Niste, J. Walker, J. Zekonyte, Mechanism of action of WS2 lubricant nanoadditives in high-pressure contacts, *Tribol. Lett.*, 2013, **52**, 81-91.

18 PCS Instruments, MTM (Mini traction Machine), Retrieved 31th of March, 2014: http://www.pcs-instruments.com/brochures.shtml#

19 Alicona, Infinite Focus Real 3D, Retrieved 31th of March, 2014: http://www.alicona.com/home/products/infinitefocus-standard.html

20 Micro Materials, Nanoindentation, Retrieved 31th of March, 2014: http://www.micromaterials.co.uk/the-nano-test/nanoindentation/

21 L. Joly-Pottuz, F. Dassenoy, M. Belin, B. Vacher, J. M. Martin, N. Fleischer, Ultralow-friction and wear properties of IF-WS2 under boundary lubrication, *Tribol. Lett.*, 2005, **18** (4), 477-484.

22 M. Ratoi, R. C. Castle, C. H. Bovington, H. A. Spikes, The influence of soot and dispersant on ZDDP film thickness and friction, *Lubr. Sci.*, 2004, **17** (1), 25 43.

23 W. C. Oliver, G. M. Pharr, An improved technique for determining hardness and elastic-modulus using load and displacement sensing indentation experiments, *J. Mater. Res.*, 1992, **7** (6), 1564-1583.

24 B. D. Beake, S. Zheng, M. R. Alexander, Nanoindentation testing of plasma-polymerised hexane films, *J. Mater. Sci.*, 2002, **37** (18), 3821-3826.

25 Z. Zhang, E. S. Yamaguchi, M. Kasrai, G. M. Bancroft, Tribofilms generated from ZDDP and DDP on steel surfaces: Part 1, growth, wear and morphology, *Tribol. Lett.*, 2005, **19** (3), 211-220.

26 L. Taylor, H. A. Spikes, Friction-enhancing properties of ZDDP antiwear additive: part I – friction and morphology of ZDDP reaction films, *Tribol. Trans.*, 2003, **46**, 303-309.

27 J. M. Palacios, Thickness and chemical composition of films formed by antimony dithiocarbamate and zinc dithiophosphate, *Tribol. Int.*, 1986, **19** (1), 35-39.

28 J. M. Palacios, Films formed by antiwear additives and their incidence in wear and scuffing, *Wear*, 1987, **114** (1), 41-49.

29 M. Ratoi, V. B. Niste, H. Alghawel, A. Suen, K. Nelson, The Impact of Organic Friction Modifiers on Engine Oil Tribofilms, *RSC Adv.*, 2014, **4**, 4278-4285.

30 R. Saha, W. D. Nix, Effects of the substrate on the determination of thin film mechanical properties by nanoindentation, *Acta Mater.*, 2002, **50**, 23-38.

31 G. Pereira, A. Lachenwitzer, M. Kasrai, G. M. Bancroft, P. R. Norton, M. Abrecht, P. U. P. A. Gilbert, T. Regier, R. I. R. Blyth, J. Thompson, Chemical and mechanical analysis of tribofilms from fully formulated oils Part 1 – Films on 52100 steel, *Tribology*, 2007, **1** (1), 48-61.

32 S. Bec, A. Tonck, J. M. Georges, G. W. Roper, Synergistic effects of MoDTC and ZDDP on frictional behaviour of tribofilms at the nanometer scale, *Tribol. Lett.*, 2004, **17** (4), 797-809.

33 A. Morina, A. Neville, M. Priest, J. H. Green, ZDDP and MoDTC interactions in boundary lubrication – the effect of temperature and ZDDP/MoDTC ratio, *Tribol. Int.*, 2006, **39**, 1545-1557.

WS$_2$ nanoparticles possess remarkable tribological and physicochemical properties which recommend them as potential candidates for replacing problematic additives.